Determination of the ω- and η'-nucleus optical potential

M. Nanova[1,⋆] and V. Metag[1]
for the CBELSA/TAPS Collaboration

[1] *II. Physikalisches Institut, Justus-Liebig Universität, Giessen, Germany*

Abstract. The ω and η'-nucleus interaction has been studied in photoproduction reactions off C and Nb targets, using the CBELSA/TAPS detector system. Transparency ratio measurements provide information on the inelastic cross section and in-medium width of mesons and thereby on the imaginary part of the meson-nucleus potential. The real part of the optical potential can be deduced from measurements of the excitation function and momentum distribution which are sensitive to the sign and depth of the potential. Data taken on a C and Nb target have been analysed to determine the real and the imaginary part of the ω- and η'-nucleus optical potential. The momentum dependence of the imaginary part of both mesons is presented and discussed. The results are compared to previous experimental results and to model calculations assuming different scenarios. The data are consistent with a weakly attractive potential for both mesons. The relatively small in-medium width of the η' meson encourages the search for η' bound states.

1 Introduction

The in-medium modifications of hadron properties have been identified as one of the key problems in understanding the non-perturbative sector of QCD. Several theoretical papers discuss the possibility of a partial restoration of chiral symmetry in a strongly interacting environment [1–3]. Mesons are considered to be excitations of the QCD vacuum which has a complicated structure with non-vanishing chiral and higher order condensates. These condensates are predicted to change within a strongly interacting medium and, as a consequence, also the mass spectrum of mesons is expected to be modified [2]. This idea inspired hadronic models developed to calculate the in-medium self-energies of hadrons and their spectral functions. Mass shifts and/or in-medium broadening as well as more complex structures in the spectral function due to the coupling of vector mesons to nucleon resonances have been predicted [4, 5].

Recently many studies have focused on the η' meson. Its especially large mass compared to the mass of the other pseudoscalar mesons has to be attributed to chiral and flavor symmetry breaking effects. Due to a reduction of the chiral condensate a drop in the $U_A(1)$ breaking part of the η' mass might be expected [6, 7], causing an η' mass shift of ≈-120 MeV at nuclear matter density ρ_0. This prediction is, however, in conflict with earlier calculations within the Nambu-Jona-Lasinio-model which expect almost no change in the η' mass as a function of nuclear density [8]. Further model calculations claim mass shift of the η' of -80, -40 MeV at ρ_0 [9, 10]. It is obvious that these contradictory theoretical predictions call for an experimental clarification.

⋆e-mail: Mariana.Nanova@exp2.physik.uni-giessen.de

2 Experimental approaches to study mesons in the medium

The meson-nucleus interaction and the in-medium modifications of mesons can be described by an optical potential

$$U(r) = V(r) + iW(r), \tag{1}$$

comprising a real (V(r)) and an imaginary (W(r)) part; r is the distance between the meson and the centre of the nucleus [6]. The strength of the real part of the meson-nucleus potential is connected to the meson in-medium mass shift $\Delta m(\rho_0)$ at saturation density ρ_0 by:

$$V(r) = \Delta m(\rho_0) \cdot c^2 \cdot \frac{\rho(r)}{\rho_0}. \tag{2}$$

The imaginary part of the potential describes the meson absorption in the medium via inelastic channels and is related to the in-medium width Γ_0 of the meson at nuclear saturation density by [11]

$$W(r) = -\frac{1}{2}\Gamma_0 \cdot \frac{\rho(r)}{\rho_0}. \tag{3}$$

The experimental approaches to determine the real part of the potential which were applied for ω and η' mesons and discussed in this paper are: (i) excitation function of the meson and (ii) meson momentum distributions.

The imaginary part of the meson-nucleus potential corresponds to half of the in-medium width: $\mathrm{Im}U = \Gamma/2$, which can be extracted from the attenuation of the meson flux deduced from a measurement of the so-called transparency ratio for a number of nuclei [12]. The transparency ratio describes the loss of flux of mesons in nuclei via inelastic processes. Due to these processes the lifetime of mesons in a nuclear medium is reduced leading to an increase in width as compared to the free particle width.

The data on ω and η' photoproduction were taken in a series of experiments in 2009 and 2013/14 with the Crystal Barrel/TAPS detector system at the ELSA accelerator in Bonn [13, 14]. The high segmentation and the almost full solid angle coverage of the detector systems allowed the reconstruction of ω and η' mesons from multi photon final states by invariant mass analysis. The decay modes used in the analyses were $\omega \to \pi^0\gamma \to 3\gamma$ and $\eta' \to \pi^0\pi^0\eta \to 6\gamma$ with branching ratios of 8.2% and 8.5%, respectively [15].

2.1 The real part of the ω- and η'-nucleus optical potential

Information on the in-medium meson mass and the real part of the meson-nucleus potential can be extracted from the excitation function of the meson as shown in [16, 17]. The experimental results for the ω excitation function in comparison to theoretical calculations are shown in Fig. 1(left). Data were taken on a carbon target with the Crystal Ball and TAPS detector system at MAMI-C. The GiBUU transport model [18] has been applied to calculate the ω excitation function for 6 different scenarios allowing for mass shifts up to -125 MeV at normal nuclear density. It is obvious that the data are not consistent with a strong mass shift scenario, $|V|$>100 MeV as predicted in [2, 19]. A χ^2-fit of the data with the excitation functions calculated for the different scenarios gives a potential depth of $V_{\omega A}(\rho = \rho_0) = -(42 \pm 17(\mathrm{stat}) \pm 20(\mathrm{syst}))$ MeV [20].

The excitation functions for η' meson produced off C and Nb appear to be incompatible with η' mass shifts of -100 MeV and more at normal nuclear matter density, as clearly seen in Fig. 1(middle and right). A χ^2-fit of the data with the excitation functions calculated for the different scenarios over

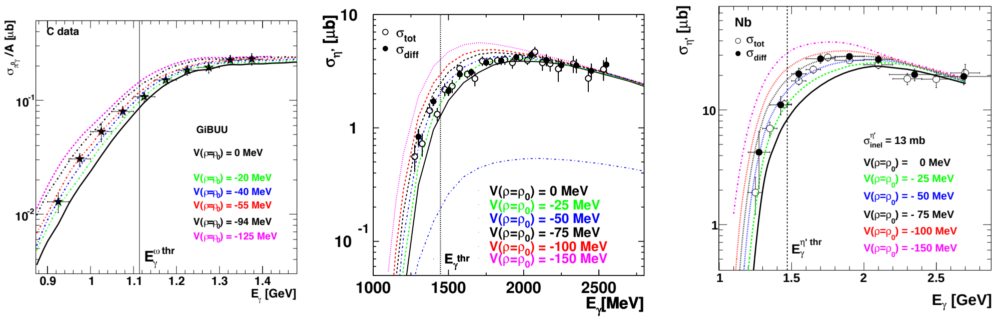

Figure 1. (Left) Measured excitation function for the ω meson in comparison to GiBUU transport calculations for several in-medium modification scenarios [20] assuming mass shifts up to -125 MeV. Measured excitation function for the η' meson off ^{12}C (middle) and ^{93}Nb (right), in comparison to theoretical calculations for different scenarios [14, 21]. The experimental data are extracted by integrating the differential cross sections (full circles) and by direct measurement of the η' yield in incident photon energy bins (open circles). The calculations are for $\sigma_{\eta' N}$=11 mb (for C data) and for $\sigma_{\eta' N}$=13 mb (for Nb data), and for potential depths: V=0 MeV (black line), -25 MeV (green), -50 MeV (blue), -75 MeV (black dashed), -100 MeV (red) and -150 MeV (magenta) at normal nuclear density, respectively, and using the full nucleon spectral function. The dot-dashed blue curve (in the middle spectrum) indicates the fraction of η' mesons produced off correlated nucleon pairs.

the full range of incident energies gives a potential depth of -(40±6) MeV and -(40±12) MeV for C and Nb, respectively [14, 21].

As discussed in [16, 17], the momentum distribution of the mesons is also sensitive to the potential depth and has been investigated as well. A χ^2-fit of the data with the momentum distributions calculated for the different scenarios gives a depth of -(32±11) MeV and -(45±20) MeV for the η'-C and η'-Nb potential, respectively [14, 21].

To study the possible momentum dependence of the real part of the meson-nucleus optical potential an experiment has been performed to produce ω mesons with low momenta (< 500 MeV/c). In the reaction $\gamma C \rightarrow \omega p \rightarrow \pi^0 \gamma p$ the proton, detected in the TAPS detector ($\Theta_p = 1° - 11°$), takes over most of the momentum of the incoming photon beam. Being so low in energy, the ω-mesons are particularly sensitive to the ω nucleus potential. In case of a strongly repulsive (attractive) interaction one would expect the peak in the kinetic energy distribution to be shifted to higher (lower) energies for the C target. The sensitivity of the peak position in the kinetic energy distribution on the potential depth, studied in [22], can be exploited to deduce the depth of the real part of the ω-nucleus potential. The experimental data for the ω kinetic energy distribution have been compared with the theoretical calculations and a potential depth of -(15±35) MeV has been determined, which appears to be too small to allow for the formation of ω mesic states in view of the large in-medium width of $\approx$ 90 MeV (see Sec. 2.2). Combining the results from the analysis of the excitation function and the peak position from the kinetic energy distribution an average depth of the real part of the ω-C optical potential of V($\rho = \rho_0$) = -(29 ±19(stat)±20(syst)) MeV is obtained Fig. 2 (left).

From the analysis of the excitation functions and the momentum distributions for the η' meson and by proper weighting of the errors a depth of the real part of the η'-C and -Nb optical potential of V($\rho = \rho_0$) = -(39 ±7(stat)±15(syst)) MeV is obtained (see Fig. 2 (right)). This result for V($\rho = \rho_0$) is consistent with predictions of the η'-nucleus potential depth within the Quark-Meson Coupling model [10] and with calculations in [23] but does not support larger mass shifts as discussed in [6, 9].

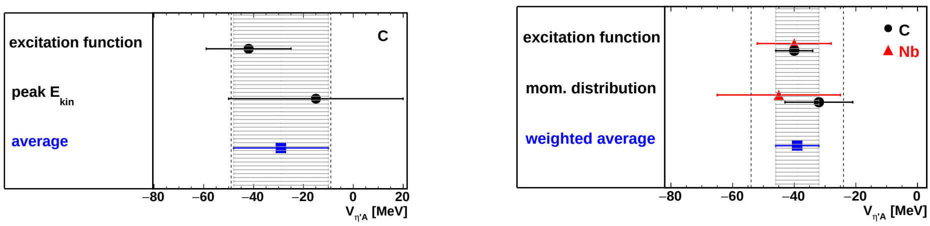

Figure 2. Depths of the real part of the ω (left) and η' (right) -nucleus potential determined by analyzing the excitation function and the momentum distributions for C [20, 21] (full black circles) and for Nb [14] (red triangles). The weighted overall average is indicated by a blue square. The shaded area indicates the statistical error. The vertical hatched lines mark the range of systematic uncertainties [14, 24].

2.2 The imaginary part of the ω- and η'-nucleus optical potential

To determine the meson attenuation in nuclei and the inelastic meson-nucleon cross sections as a function of the meson momentum, the transparency ratio is deduced from the data as defined in Eq.4 [11, 13, 25]. To suppress nuclear effects not related to meson absorption, the transparency ratio is not taken relative to the free nucleon but rather to a nucleon in a light nucleus like carbon. The momentum dependence of the transparency ratio for a meson m is thus obtained by dividing the differential inclusive meson production cross sections for niobium by the one for carbon according to Eq.4

$$T^{\mathrm{m}}_{\mathrm{Nb/C}}(p_m) = \frac{12 \cdot \frac{d\sigma_{\gamma \mathrm{Nb} \to \mathrm{mX}}}{dp_m}(p_m)}{93 \cdot \frac{d\sigma_{\gamma \mathrm{C} \to \mathrm{mX}}}{dp_m}(p_m)}, \tag{4}$$

where 12 and 93 are the nuclear mass numbers of carbon and niobium, respectively. The resulting transparency ratios as a function of the meson momentum are shown in Fig. 3. Consistent with earlier measurements [21, 25], a slight increase with momentum is observed for the ω meson while for the η' meson the transparency ratio is almost independent of momentum. The momentum depen-

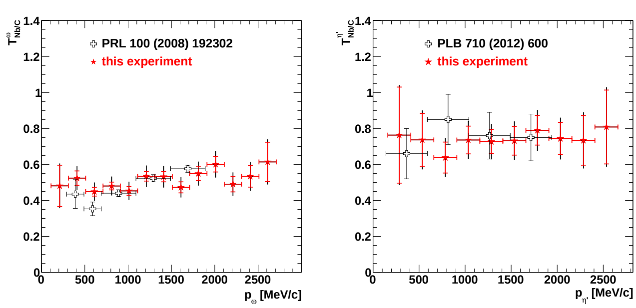

Figure 3. The transparency ratio according to Eq. 4 for (Left) ω and (Right) η' photoproduction off carbon and niobium (red stars) in comparison to earlier measurements (open crosses) [11, 25]. For the present data the thick error bars (red) represent the statistical errors. The thin error bars (black) include the systematic errors added in quadrature [13].

dence of the transparency ratio allows the determination of the in-medium ω and η' widths which can be converted into the dependence of the imaginary part of the ω- and η'-nucleus potential as a function of the available energy in the meson-^{93}Nb system, as shown in Fig. 4 (for more details see [13]). The data have been fitted and extrapolated towards the production threshold. For the ω meson the modulus of the imaginary part of the meson nucleus potential near threshold is found to be (48 ± 12(stat)± 9(syst)) MeV comparable to the modulus of the real part of about 30 MeV, determined in [20, 22, 27]. For the η' meson the extrapolation towards the production threshold yields an imaginary potential of (13 ± 3(stat)±3(syst)) MeV, corresponding to an imaginary part of the η' scattering length Im($a_{\eta' N}$) = (0.16 ± 0.05) fm. This is about a factor two smaller than obtained in the direct determination of the $\eta' N$ scattering length from an analysis of near threshold η' production in the $pp \to pp\eta'$ reaction [28], but almost overlaps within the errors.

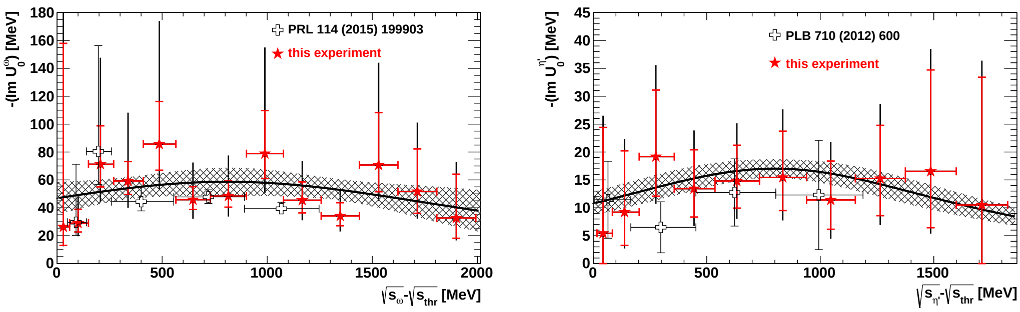

Figure 4. Imaginary part of the (Left) ω-nucleus and (Right) η'-nucleus optical potential as a function of the available energy in the meson-^{93}Nb system (red stars) [13] in comparison to earlier measurements (open crosses) [11, 25, 26]. The solid curves are Breit-Wigner fits to the present data. The shaded areas indicate a confidence level of $\pm 1\sigma$ of the fit curve taking statistical and systematic errors into account (taken from [13]).

3 Conclusion

The photoproduction of ω and η' mesons off nuclei has been studied in the 1-3 GeV energy range to extract information on the in-medium properties of these mesons. The interaction of mesons with nuclei and the in-medium effects have been described with an optical model, comprising a real part, associated with the mass modification in the nuclear medium, and an imaginary part, accounting for the absorption of mesons in nuclei. For the ω- and η'- nucleus optical potential values of $U_{\omega A}(\rho = \rho_0)$ = -((29 ±19(stat)±20(syst)) + i(48±12(stat)±9(syst))) MeV and $U_{\eta' A}(\rho = \rho_0)$ = -((39 ±7(stat)±15(syst)) + i(13±3(stat)±3(syst))) MeV have been obtained (Fig. 5) [24]. The latter measurement establishes an in-medium mass drop of a pseudoscalar meson at normal nuclear matter density. Although not very deep, the real part of the η' - nucleus potential is about three times larger than the imaginary part and may thus allow the existence and observation of η'-nucleus states, only bound by the strong interaction. Corresponding experiments are ongoing.

4 Acknowledgements

We would like to thank our coworker Stefan Friedrich as well as all other colleagues in the CBELSA/TAPS collaboration for important contributions to this work. This work is supported by the *Deutsche Forschungsgemeinschaft* within SFB/TR16.

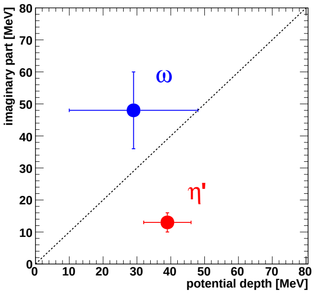

Figure 5. The imaginary part versus the real part of the meson-nucleus potential for ω and η' mesons [24].

References

[1] V. Bernard and U.-G. Meissner, Nucl. Phys. A **489**, 647 (1988)
[2] T. Hatsuda and S. Lee, Phys. Rev. C **46**, R34 (1992)
[3] G. E. Brown and M. Rho, Phys. Rev. Lett. **66**, 2720 (1991)
[4] P. Mühlich et al., Nucl. Phys. A **780**, 187 (2006)
[5] M. Lutz *et al.*, Nucl. Phys. A **706**, 437 (2002)
[6] H. Nagahiro, M. Takizawa, and S. Hirenzaki, Phys. Rev. C **74**, 045203 (2006)
[7] Y. Kwon *et al.*, Phys. Rev. D **86**, 034014 (2012)
[8] V. Bernard and U.-G. Meissner, Phys. Rev. D **38**, 1551 (1988)
[9] S. Sakai and D. Jido, Phys. Rev. C **88**, 064906 (2013)
[10] S. D. Bass and A. W. Thomas, Phys. Lett. B **634** 368 (2006)
[11] M. Nanova *et al.*, CBELSA/TAPS Collaboration, Phys. Lett. B **710**, 600 (2012)
[12] D. Cabrera *et al.*, Nucl. Phys. A **733**, 130 (2004)
[13] S. Friedrich *et al.*, CBELSA/TAPS Collaboration, Eur. Phys. J. A **52**, 297 (2016)
[14] M. Nanova *et al.*, CBELSA/TAPS Collaboration, Phys. Rev. C **94**, 025205 (2016)
[15] K. A. Olive *et al.*, Particle Data Group, Chin. Phys. C **38**, 090001 (2014)
[16] J. Weil, U. Mosel, and V. Metag, Phys. Lett. B **723**, 120 (2013)
[17] E. Ya. Paryev, J. Phys. G: Nucl. Part. Phys. **40**, 025201 (2013)
[18] O. Buss *et al.*, Phys. Rep. **512**, 1 (2012)
[19] F. Klingl *et al.*, Nucl. Phys. A **610**, 297 (1997), Nucl. Phys. A **650**, 299 (1999)
[20] V. Metag *et al.*, A2 Collaboration, Prog. Part. Nucl. Phys. **67**, 530 (2012)
[21] M. Nanova *et al.*, CBELSA/TAPS Collaboration, Phys. Lett. B **727**, 417 (2013)
[22] S. Friedrich *et al.*, CBELSA/TAPS Collaboration, Phys. Lett. B **736**, 26 (2014)
[23] H. Nagahiro, S. Hirenzaki, E. Oset, and A. Ramos, Phys. Lett. B **709**, 87 (2012)
[24] V. Metag, M. Nanova, and K.-T. Brinkmann, CRC 16 Symp., Proceed. June (2016)
[25] M. Kotulla *et al.*, CBELSA/TAPS Collaboration, Phys. Rev. Lett. **100**, 192302 (2008)
[26] M. Kotulla *et al.*, CBELSA/TAPS Collaboration, Phys. Rev. Lett. **114**, 199903 (2015)
[27] V. Metag, Hyp. Int. **234**, 25 (2015)
[28] E. Czerwinski *et al.*, Phys. Rev. Lett. **113**, 062004 (2014)